Patterns of particle distribution in multiparticle systems by random walks with memory enhancement and decay

Zhi-Jie Tan, Xian-Wu Zou,* Sheng-You Huang, Wei Zhang, and Zhun-Zhi Jin
Department of Physics, Wuhan University, Wuhan 430072, China
(Received 30 January 2002; published 8 July 2002)

We investigate the pattern of particle distribution and its evolution with time in multiparticle systems using the model of random walks with memory enhancement and decay. This model describes some biological intelligent walks. With decrease in the memory decay exponent α, the distribution of particles changes from a random dispersive pattern to a locally dense one, and then returns to the random one. Correspondingly, the fractal dimension $D_{f,p}$ characterizing the distribution of particle positions increases from a low value to a maximum and then decreases to the low one again. This is determined by the degree of overlap of regions consisting of sites with remanent information. The second moment of the density $\rho^{(2)}$ was introduced to investigate the inhomogeneity of the particle distribution. The dependence of $\rho^{(2)}$ on α is similar to that of $D_{f,p}$ on α. $\rho^{(2)}$ increases with time as a power law in the process of adjusting the particle distribution, and then $\rho^{(2)}$ tends to a stable equilibrium value.

DOI: 10.1103/PhysRevE.66.011101 PACS number(s): 05.40.−a, 87.18.Bb, 61.43.Hv

I. INTRODUCTION

During the last two decades, the collective motion of particles in complex systems has attracted considerable interest [1–3]. Recently, there has been increasing interest in research into biological motions, such as the migration of fish, flocks of flying birds, animal grouping habits, and the collective behavior of robots [4–7]. In these phenomena, the action of each individual is independent and random, but they tend to become cooperative and grouped. Great effort has been put into modeling and simulating the collective behavior of elements, such as animals, insects, and robots [8–10]. Vicsek *et al.* introduced a model to describe the self-ordered motion of biological individuals, in which the velocity of a given particle is related to those of the neighbor particles [8,9]. Shimoyama *et al.* proposed a mathematical model for the collective motion in a system with mobile elements [10]. The model shows several kinds of cluster motion, including collective rotation, chaos, and wandering. These dynamical models can give pictures of the cooperative motion for multiparticle systems, but the interactions between particles are somewhat unnatural.

Recently, other kinds of effort have been made to investigate the motion behavior in the insect and animal worlds, based on a random walk with interactions. Several kinds of random walk with interactions have been proposed, including the active walk, self-attracting walk (SATW), ''true'' SATW, and so on [11–16]. In the SATW model, a random walker jumps to the nearest neighbor sites with jumping probability $p \propto \exp(nu)$, where $n=1$ for already visited sites and $n=0$ for unvisited sites [12–14]. u stands for the attractive interaction. For $u>0$, the walk is attracted to its own trajectory. The ''true'' SATW model is an extended version of the original SATW. This model involves the enhancement of n with increase of visited times [14,15]. In our very recent work, considering the character of biological walks, we presented a model of a random walk with memory enhancement and decay, i.e., the memory information increases with visited times and decays with time [17]. To our knowledge, not much attention has been paid to random walks with interaction in multiparticle systems [11,18].

In this paper, we investigate the evolution of the particle distribution with time and the dependence of the particle distribution upon the memory decay exponent in multiparticle systems, based on random walks with memory enhancement and decay. The results will be helpful to understand the motion behaviors of particles in complex systems with interactions between the elements and the environment, such as the behaviors of insects, animals, and the collective motion of robots.

II. MODEL AND METHOD

The initial system is a square lattice, on which particles are randomly placed. The movement of particles is limited by the rules of random walk with memory enhancement and decay [17]. According to this model, the movements of the particles are controlled both by randomness and by the amount of information at the lattice sites. In other words, the particle walks randomly in nature and has a preference for moving to a place with larger amount of information, something like the way an ant finds its way home by the scent which it left. The whole of the information on the lattice can be described by a field. It is named the information field (potential). For the ant, the information field presents the distribution of the scent at all sites.

Monte Carlo (MC) simulations were used to investigate the motion of the walker. The MC step is chosen as the time unit. In the walk, when a site i is visited once the information amount s_i at the site i will increase by 1. At the same time, the increased information attenuates exponentially with a non-negative memory decay exponent α. Therefore, at the site i the information amount $s_i(t)$ at the time t is the accu-

*Author to whom correspondence should be addressed. Email address: xwzou@whu.edu.cn

mulation of the remanent information at each time step. We have

$$s_i(t) = \sum_{t_0=1}^{t} n_i(t_0) e^{-\alpha(t-t_0)}, \tag{1}$$

where $n_i(t_0)$ is taken as 1 (if the site i was visited at time t_0) or 0 (if the site i was not visited at time t_0). Therefore, the probability p_{ij} with which the walker jumps from site i to its neighbor site j depends on the difference between the information amount at the site i and that at the site j. It is expressed by

$$p_{ij} \propto \exp\{\beta(s_j - s_i)\}, \tag{2}$$

where β is formulated as a Boltzmann factor. Since the physical temperature does not play any role in this abstract model, we take $\beta = 1$. Thus Eq. (2) can be rewritten as

$$p_{ij}(t) \propto \exp\left\{ \sum_{t_0=1}^{t} [n_j(t_0) - n_i(t_0)] e^{-\alpha(t-t_0)} \right\}. \tag{3}$$

The above model established for a single particle is suitable for a multiparticle system, as we consider that the information is contributed by all particles. Since there is an upper limit in sensitive volume for the smell of insects and animals, excessive smell is useless. For convenience we introduce a cutoff s_m. The restriction on s can be described as

$$s(t) \leqslant s_m. \tag{4}$$

As the memory decay exponent α takes the limiting values, this model reduces to the corresponding random walk in a multiparticle system. For instance, when $\alpha = 0$, the information never declines and the present model reduces to the SATW of a multiparticle system, and when $\alpha \to \infty$ the model degenerates to pure random walks of multiple particles.

III. RESULTS AND DISCUSSION

Numerical simulations are performed on a finite square lattice of $L \times L$. L is the length of the lattice. The length of the square particles is chosen to be the unit of length. The average particle density is given by $\rho_0 = N/L^2$, where N is the total number of particles. In this work, attention is focused on the distribution pattern of the particle positions. The average particle density is taken as small ($\rho_0 < 0.1$). The size of the square lattice is chosen to be 200×200. To reduce fluctuations, all the results are taken from averaging over five independent runs.

Two-dimensional simulations are performed for various memory decay exponents α, particle densities ρ_0, and information cutoffs s_m. Here, s_m takes small values because the initial stage of the simulation will become very long for large s_m [12,14,15].

We simulate the distribution of particles, that move by random walks with memory enhancement and decay for a set of α at the average particle density $\rho_0 = 0.02$, 0.04, and 0.08. Figure 1 shows the variation of the information distribution and particle distribution with the memory decay exponent α at $\rho_0 = 0.02$. The region with the remanent information is called the information region for short. In the simulations we take $s > 10^{-7}$ instead of $s > 0$ as the standard to judge whether the remanent information exists or not. In Fig. 1, the information region is symbolized by gray areas. It can be

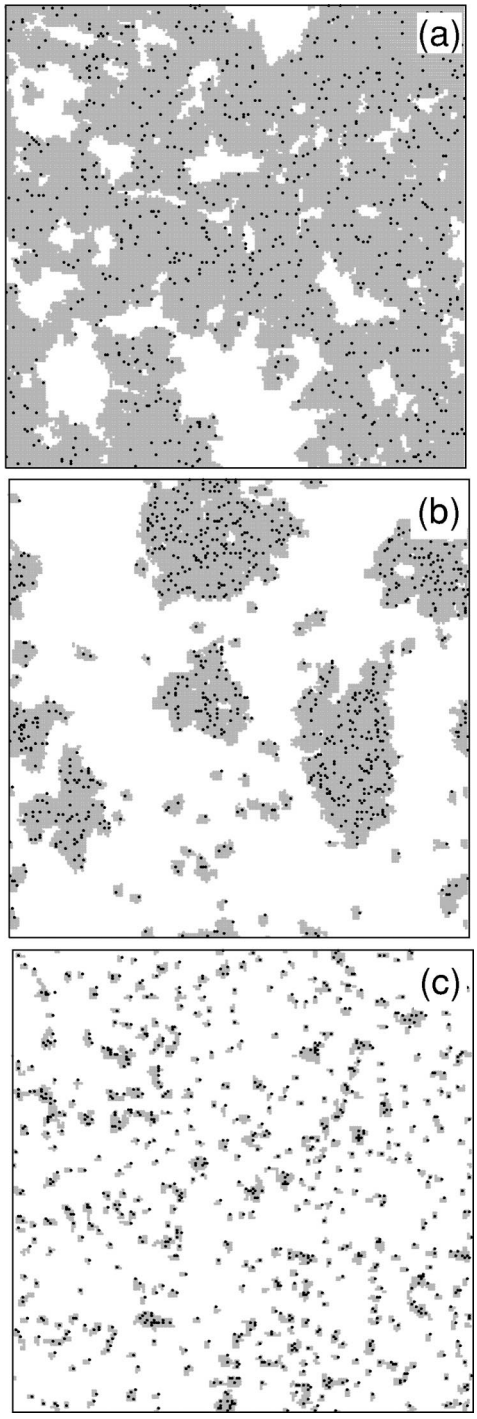

FIG. 1. Patterns of information distribution and particle distribution. The particles move by random walks with memory enhancement and decay. The average particle density $\rho_0 = 0.02$. The information cutoff $s_m = 4$. The time $t = 2 \times 10^6$. The memory decay exponent $\alpha = 0.01$ (a), 0.002 (b), and 0.0005 (c). The particles are denoted by black points. The sites with the remanent information are plotted as gray areas.

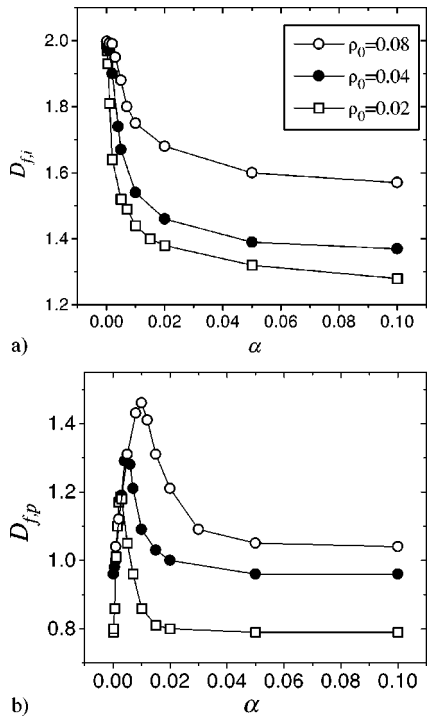

FIG. 2. Fractal dimensions of the information regions $D_{f,i}$ (a) and of the particle distributions $D_{f,p}$ (b) as a function of the memory decay exponent α. The information cutoff $s_m=4$. The time $t=2\times10^6$. The average particle density $\rho_0=0.08$ (open circles), 0.04 (full circles), and 0.02 (open squares).

seen that for very small α [see Fig. 1(a)] the information decays only slightly, so the sites with remanent information are joined together. These sites form a single continuous information region and there are some regions without information inside. In this case, the particles disperse randomly in the continuous information region. With increasing α, the information obviously decays; thus the sites with remanent information form separate information regions with various sizes and the particles are distributed randomly in them, as shown in Fig. 1(b). For large α [see Fig. 1(c)], the information decays seriously. In this case, the information regions are very small in size and spread over the whole lattice. The particles spread randomly also.

The variations of the information distribution and particle distribution with α at $\rho_0=0.04$ and 0.08 are analogous to those at $\rho_0=0.02$, but for the higher average particle density the particles in the information regions are denser and the single continuous information region starts to appear at smaller α.

To describe the information distribution and particle distribution quantitatively, we calculated the fractal dimensions of the information regions $D_{f,i}$ and those of the morphology of the particle distribution $D_{f,p}$. These are calculated by the box-counting method [19,20]. Here, the fractal dimension only in a sense characterizes the distribution of particle positions, and it does not imply that the particle distribution is scale invariant. Figures 2(a) and 2(b) plot $D_{f,i}$ and $D_{f,p}$ as a function of the memory decay exponent α at various particle densities ρ_0. Figure 2 can be explained as follows. When the decay exponent $\alpha=0$, the information does not decay. The information account s for all sites will reach s_m, and the fractal dimension of the information region $D_{f,i}=2.0$, as expected [see Fig. 2(a)]. In this case, the motion of the particles reduces to purely random walks on the whole square lattice. Thus, the fractal dimension of the particle distribution $D_{f,p}$ takes a small value corresponding to that of the randomly distributed particles at given average particle density [see Fig. 2(b)], which is consistent with Ref. [19]. What will happen as α increases slightly? In this case, the information decays slightly and some regions without information are inserted in the continuous information region [see Fig. 1(a)]. Therefore, the fractal dimension of the information region $D_{f,i}$ decreases, as shown in Fig. 2(a). Since the particles are located in the information region and the area of the information region is reduced, the average density of particles increases. It is well known that increasing the average density of particles brings about an increment of the fractal dimension of randomly placed particles [19]. Thus, we expect that the fractal dimension characterizing the distribution of particle positions $D_{f,p}$ will increase. With increasing α the area of the continuous information region is reduced, and the area and number of regions without information increase, so $D_{f,i}$ decreases. In this case, $D_{f,p}$ is governed by two factors. On the one hand, the increment of the average density of particles makes $D_{f,p}$ increase, and on the other hand the damage to the information region in which the particles are contained leads to a reduction in $D_{f,p}$. When α is close to a certain value α_p, the regions without information are connected with each other, and the information regions are separated from each other [see Fig. 1(b)]. Thus, $D_{f,p}$ reaches the maximum $(D_{f,p})_{max}$ as seen in Fig. 2(b). After that, as α continues increasing, the number of the information regions increases, the average area per information region becomes smaller and smaller, and the information regions tend toward a random distribution. Therefore, $D_{f,i}$ continues decreasing. Since the information regions in which the particles are located tend to a random distribution with increasing α, $D_{f,p}$ decreases too. When $\alpha\rightarrow\infty$, the information attenuates so fast that only the sites occupied by particles have the information amount of one unit and the rest have no information. The pattern in Fig. 1(c) is close to this situation. Thus, the motion of particles is not affected by the surroundings and it corresponds to purely random walks. In this case, both the fractal dimensions $D_{f,i}$ and $D_{f,p}$ have the same value as that of randomly distributed particles on a two-dimensional lattice. Figure 2 also shows that $D_{f,i}$ and $D_{f,p}$ get larger with increasing ρ_0. The reason is that the larger density of particles causes a denser distribution of both information regions and particles. This results in larger $D_{f,i}$ and $D_{f,p}$ [19]. In addition, the peak positions in the $D_{f,i}$-α and $D_{f,p}$-α curves shift in the direction of large α, along with increasing ρ_0.

To investigate the density nonuniformity of particle distributions quantitatively, we introduce the second moment of the density $\rho^{(2)}$. Dividing the square lattice into M cells with the same size, $\rho^{(2)}$ is defined as

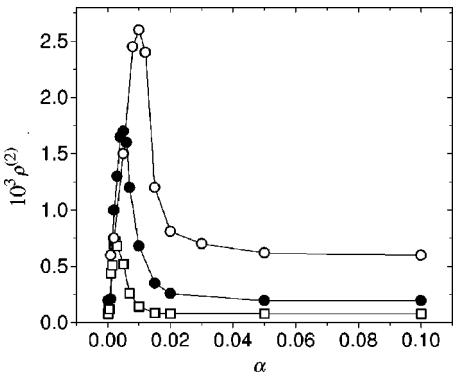

FIG. 3. The second moment of the density $\rho^{(2)}$ as a function of the memory decay exponent α. The information cutoff $s_m=4$. The time $t=2\times10^6$. The average particle density $\rho_0=0.08$ (open circles), 0.04 (full circles), and 0.02 (open squares).

$$\rho^{(2)}=\frac{1}{M}\sum_{i=1}^{M}\langle\rho_i-\rho_0\rangle^2, \tag{5}$$

where ρ_i is the particle density of the ith cell. The plots of $\rho^{(2)}$ versus α for a set of ρ_0 are shown in Fig. 3. The relation of $\rho^{(2)}$ to α is very similar to that of $D_{f,p}$ to α. It can be explained as follows. $\rho^{(2)}$ describes the density nonuniformity of the particle distribution in a system. When $\alpha\to\infty$, the information regions degenerate into the sites occupied by particles, so the distribution of particles is random, and $\rho^{(2)}$ takes a small value depending on ρ_0. With decreasing α, the information regions get larger and larger, and the neighboring information regions join together. The particles are located in these information regions, so that the nonuniformity of the particle distribution is enhanced and $\rho^{(2)}$ increases. As α continues decreasing, smaller information regions are joined up with each other and form larger information regions. Correspondingly, $\rho^{(2)}$ reaches its maximum $\rho^{(2)}_{max}$ at $\alpha=\alpha_p$, and then $\rho^{(2)}$ decreases. When α is very small, all the information regions are joined together and form a single continuous region which spreads all over the lattice, and the particles move randomly in the lattice. Thus, $\rho^{(2)}$ returns to a small value at $\alpha=0$.

To investigate the effect of the information cutoff s_m on the distribution of particles, simulations with $s_m=4$ and 6 were performed. It was found that, as s_m increases from 4 to 6, $\rho^{(2)}_{max}$ decreases from 5.4×10^{-4} to 5.0×10^{-4} for $\rho_0=0.02$. Meanwhile, α_p is reduced from 0.0025 to 0.0006. These results are easy to understand. For larger s_m, the attracting ''trap'' is deeper, so it is more difficult for the particles to escape from their trap and join up with the neighboring information regions [14,15]. This brings about a decrease of the nonuniformity of the particle distribution. This means that $\rho^{(2)}_{max}$ is reduced as s_m increases. In addition, a smaller α corresponds to weaker decay of information, and the weaker decay is favorable for the particle escaping from the trap and for joining of neighboring information regions, so α_p takes a smaller value for larger s_m to obtain the maximum nonuniformity of the particle distribution $\rho^{(2)}_{max}$.

Now, we turn to evaluation of the transition point from the dense phase to the dispersive one for the pattern of the particle distribution. Figures 1 and 2 show that as long as the decay exponent is larger than a certain small value (say 10^{-3}, for $\rho_0=0.02$) the pattern is dense, and then it becomes dispersive as α increases a little. The transition takes place in a narrow range of α. The transition point α_c can be evaluated roughly as follows. As a particle moves, an information region is generated around it. When the information regions generated by near neighboring particles overlap enough, the pattern of the particle distribution is dense; otherwise it is dispersive. For the present systems with low particle density ($\rho_0<0.1$), the motion of each particle can be described by the SATW of a single particle in a first approximation. The visited sites in the SATW correspond to the information generated by the particle. For the SATW, in the case of $u>u_c$ the cluster consisting of visited sites is a compact Eden one [20–23]. Thus, the average number of visited sites $\langle S(t)\rangle$ scales with the time step t as [12–15]

$$\langle S(t)\rangle\simeq At^{2/3} \quad \text{or} \quad t\simeq[\langle S(t)\rangle/A]^{3/2}, \tag{6}$$

where A is a proportionality constant. In this multiparticle system the average area per particle is $L^2/N=1/\rho_0$. Thus, the average time t_c during which the particle moves over this area can be calculated using Eq. (6), and we have

$$t_c\simeq(A\rho_0)^{-3/2}. \tag{7}$$

At the time t_c, the information has decayed by $e^{-\alpha t_c}$. We suppose that as the remanent information is e^{-1} times less than the initial information, the information regions generated by near neighboring particles are separated, and the pattern of the particle distribution is dispersive. Therefore the transition point α_c can be expressed by

$$\alpha_c t_c=1 \quad \text{or} \quad \alpha_c=(A\rho_0)^{3/2}, \tag{8}$$

where A is somewhat related to s_m and u_c [14,15]. In this case ($s_m=4$, and correspondingly $u_c=0.5$), we simply take $A=1$. According to Eq. (8), we roughly evaluate $\alpha_c=0.003$, 0.008, and 0.023, corresponding to $\rho_0=0.02$, 0.04, and 0.08, respectively. They are in accord with the simulation results [see Fig. 2(b)].

Moreover, the evolution of the particle distribution with time was investigated for multiparticle systems with memory enhancement and decay. Figure 4 shows the dependence of the second moment of the density $\rho^{(2)}$ on time t for a system with $\rho_0=0.02$. It can be seen that the variation of $\rho^{(2)}$ with t follows a power law before $\rho^{(2)}$ reaches the stable value $\rho^{(2)}_s$. For a given value of the decay exponent α, with increasing time $\rho^{(2)}$ varies from a small value (corresponding to the random distribution) to the stable value $\rho^{(2)}_s$ (corresponding to the dynamic equilibrium distribution). $\rho^{(2)}_s$ is related to ρ_0. The evolution time t_e, i.e., the time needed to evolve from a random distribution to the equilibrium one, depends on ρ_0 also. As α rises, $\rho^{(2)}_s$ and t_e increase. The difference in the evolution behaviors of the particle distribution for systems with various α stems from the degree of overlap of information regions generated by near neighboring particles. When α is very small, the overlapping parts

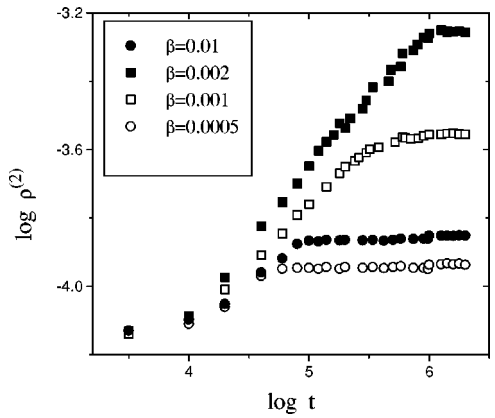

FIG. 4. The evolution of the second moment of the density $\rho^{(2)}$ with time for several memory decay exponents α. The information cutoff $s_m=4$. The average particle density $\rho_0=0.02$.

generated by near neighboring particles are very large and the information regions generated by all particles almost cover the lattice. In this case, the particle distributions before and after evolution are similar, so equilibrium is achieved quickly and t_e is small. In contrast, when α is large, the overlapping parts of the information regions are small and the correlation among the particles is weak. In this case, the particle distributions before and after evolution are alike again and t_e is small too. At a certain value of $\alpha=\alpha_p$, the overlap of the information regions generated by near neighboring particles is just the right amount. It results in a continuous information region, which is interspersed with non-information regions. In this case, the motions of particles are correlated with each other and there exists a large difference between the particle distributions before and after evolution. It takes much time to achieve equilibrium, so t_e reaches a maximum.

IV. CONCLUSION

In summary, for multiparticle systems with memory enhancement and decay, as the memory decay exponent α decreases, the distribution of particles changes from a random dispersive pattern to a locally dense one, and then returns to the random dispersive one. The change in the pattern comes from the fact that the motion of particles leaves information at visited sites and the particles prefer to visit the remembered sites at which information remains. When α is very large, the overlap of information regions generated by near neighboring particles is very small, so the motion of each particle is almost like a pure random walk. When α is very small, all the information region generated by each particle join together and spread all over the lattice. Thus, the particles also randomly walk over the range of the lattice. At a certain value of α, some of the information regions generated by near neighboring particle overlap and some do not. Therefore the particles are decentralized in the continuous information regions and the pattern of the particle distribution is locally dense.

ACKNOWLEDGMENT

This work was supported by the National Natural Science Foundation of China.

[1] P. Meakin, *Fractals, Scaling and Growth Far From Equilibrium* (Cambridge University Press, Cambridge, England, 1998).
[2] T. Vicsek, *Fractal Growth Phenomena* (World Scientific, Singapore, 1992).
[3] *Fractals and Disordered Systems*, edited by A. Bunde and S. Havlin (Springer, Berlin, 1991).
[4] B. Holldobler and E. O. Wilson, *The Ants* (Springer, Berlin, 1990); E. Bonabeau and G. Theraulaz, Sci. Am. **282** (3), 73 (2000).
[5] M. J. B. Krieger, J.-B. Billeter, and L. Keller, Nature (London) **406**, 992 (2000).
[6] J. K. Parrish and L. Edelstein-Keshet, Science **284**, 99 (2000); R. K. Cowen, K. M. M. Lwiza, S. Sponaugle, C. B. Paris, and D. B. Olson, *ibid.* **287**, 857 (2000).
[7] S. Wohlgemuth, B. Ronacher, and R. Wehner, Nature (London) **411**, 795 (2001).
[8] T. Vicsek, A. Czirok, E. Ben-Jacob, I. Cohen, and O. Shochert, Phys. Rev. Lett. **75**, 1226 (1995).
[9] A. Czirok and T. Vicsek, Physica A **281**, 17 (2000).
[10] N. Shimoyama, K. Sugawara, T. Mizuguchi, Y. Hayakawa, and M. Sano, Phys. Rev. Lett. **76**, 3870 (1996).
[11] *Introduction to Nonlinear Physics*, edited by L. Lam (Springer-Verlag, New York, 1997).
[12] V. B. Sapozhbikiv, J. Phys. A **27**, L151 (1994); **37**, 3935 (1998).
[13] A. Ordemann, G. Berkolaiko, S. Havlin, and A. Bunde, Phys. Rev. E **61**, R1005 (2000); **64**, 046117 (2001); A. Ordemann, Ph.D. dissertation, University of Giessen, Germany, 2001.
[14] Z. J. Tan, Ph.D. thesis, Wuhan University, Wuhan, China, 2001.
[15] Z. J. Tan, X. W. Zou, W. Zhang, and Z. Z. Jin, Phys. Lett. A **289**, 251 (2001).
[16] S. Y. Huang, X. W. Zou, W. B. Zhang, and Z. Z. Jin, Phys. Rev. Lett. **88**, 056102 (2002).
[17] Z. J. Tan, X. W. Zou, S. Y. Huang, W. Zhang, and Z. Z. Jin, Phys. Rev. E **65**, 041101 (2002).
[18] D. Amarie, C. Gherman, and M. Ignat, Phys. Lett. A **271**, 65 (2000).
[19] D. A. Hamburger, O. Biham, and D. Avnir, Phys. Rev. E **53**, 3342 (1996).
[20] Z. J. Tan, X. W. Zou, and Z. Z. Jin, Phys. Rev. E **62**, 8409 (2000).
[21] Z. J. Tan, X. W. Zou, and Z. Z. Jin, Phys. Lett. A **282**, 121 (2001).
[22] M. Eden, in *Proceedings of the Berkeley Symposium on Mathematical Statistics and Probability*, edited by J. Neyman (University of California Press, Berkeley, CA, 1961), pp. 223–239; see also Refs. [1,2].
[23] Z. J. Tan, X. W. Zou, S. Y. Huang, and Z. Z. Jin, J. Phys. Soc. Jpn. **70**, 3251 (2001).